Wojcieszak and Wadley *Herit Sci* (2019) 7:24
https://doi.org/10.1186/s40494-019-0267-9

Heritage Science

RESEARCH ARTICLE Open Access

A Raman micro-spectroscopy study of 77,000 to 71,000 year old ochre processing tools from Sibudu, KwaZulu-Natal, South Africa

Marine Wojcieszak* and Lyn Wadley

Abstract

Many Middle Stone Age sites in South Africa yielded hundreds, even thousands, of ochre pieces sometimes showing use traces. Less attention has been paid to the tools used for their processing. Here, seven tools excavated from the oldest layers (71,000 to 77,000 years ago) of Sibudu rock shelter were studied non-invasively to identify the micro-residues on them. The tools were first examined with optical microscopy to detect areas of interest. Then, Raman micro-spectroscopy was performed on the residues present, as well as on random areas of tool surfaces. These Raman signatures were compared to those obtained from the sediments and ochre samples recovered from the same layers. All tools exhibited red, orange and brown stains on their surfaces and these comprised iron oxides (haematite and maghemite) and oxyhydroxide (goethite). The other compounds detected include amorphous carbon, quartz, anatase and manganese oxides. All of these can occur within ochre, but they may alternatively be natural components of other rocks and sediments, formed secondarily by decay processes. However, the large and thick residues present on the surfaces of the artefacts imply their use for ochre processing (microscopic observations and chemical analyses of the sediments and the local rocks showed that they contain only traces of haematite). Ochre seems to have been the only material processed with these old Sibudu artefacts whereas in younger occupations, items such as bone were also processed with grindstones. The grinding tools are morphologically varied and the ochre pieces are both morphologically and chemically diverse.

Keywords: Residues, Grindstones, Ochre, Middle Stone Age, Raman micro-spectroscopy

Introduction

Pieces of ochre, especially red ones [1], are commonly found alongside stone tools and other artefacts in African Stone Age archaeological sites; these pieces often show use traces and were brought to the sites which demonstrates ochre's importance to early societies. Ochre definitions can vary depending on the field of study (for example, geology, archaeology or chemistry), its use and the period when it was used. Ochre is defined here as a geological product containing iron oxide and/or oxyhydroxides and occurring in rocks such as shales, sandstones, mudstones and specularite. The iron oxides and oxyhydroxides present in ochre are, for example, haematite, goethite, and magnetite, and the secondary compounds are minerals associated with rocks such as quartz, clay, and mica. It also leaves a coloured streak when rubbed against a harder material [2–5]. Some ochre fragments from Middle Stone Age occupations bear use traces of rubbing, grinding, scoring or what appears to be deliberate engraving [6, 7]. Grinding and scoring produce powder suitable for multiple uses. Archaeologists have hypothesised functional and symbolic uses for ochre products. A functional example is ochre powder rubbed on animal hide for tanning the leather and protecting it from bacterial action [8, 9]. Ochre can additionally be used as medicine by humans since it arrests haemorrhages and has antiseptic and astringent properties [10–12]. Ochre traces on the medial and distal part of Middle Stone Age stone tools suggest that the powder was also a component of adhesive recipes for hafting

*Correspondence: marine.wojcieszak@gmail.com
Evolutionary Studies Institute (ESI), University of the Witwatersrand, Johannesburg 2050, South Africa

[13, 14]. Many innovative Middle Stone Age technologies using ochre have been discovered in South Africa, including for example, a milk and ochre paint mixture at Sibudu [15] and a liquid ochre paint, traces of which were found in an abalone shell at Blombos [16]. Red ochre and its products can have symbolic meaning [1]. Red powder is still used ritualistically by Namibian Ovahimba who mix it with clarified butter to decorate themselves, as well as to protect their bodies against sun, insects and cold [17]. Red ochre was furthermore used to create what some archaeologists think was the first human drawing [18], and engraving on ochre surfaces is thought to represent symbolic behaviour [6]. Ochre has furthermore been used worldwide as a pigment for rock art paintings and Southern Africa yields one of the world's largest bodies of rock art which were produced by Later Stone Age communities [19].

The large rock shelter forming the Sibudu archaeological site is located near the eastern coast of South Africa in KwaZulu-Natal (Fig. 1a) [20]. Sibudu accumulated 2.7 m of anthropogenic Middle Stone Age sediments dating from 77,000 to 38,000 years ago (Fig. 1b) [20, 21]. During Wadley's excavations from 1998 to 2011 at Sibudu, an assemblage of 9286 ochre pieces was recovered from Middle Stone Age layers [22]. The pieces include a wide range of colours (shades of red, purple, orange, yellow to brown and grey) and rock types (for example, shale, mudstone, siltstone, sandstone, clay and dolerite), but bright red shale is the most common type through the sequence. It has been observed [22] that the pre-Still Bay layers (71–77,000 year old) yielded fewer ochre pieces than elsewhere in the Sibudu sequence, but those found with utilisation marks are predominantly bright red (44%) or brownish-red (28%). In contrast, the unutilised pieces are primarily orange (~ 30%). By 71,000 years ago (Still Bay layers) the majority of the pieces were clayey and mostly bright-red (~ 53%). Ochre variability and use have been widely described at Sibudu and other Middle Stone Age sites, but less is known about the tools used to process the material. A Raman micro-spectroscopy study of ~ 58,000 year old grindstones from Sibudu identified residues of red ochre (haematite) alongside bone and other organic matter so people in the younger Middle Stone Age of the site seem to have processed many types of material with grindstones [23]. Raman spectroscopy is a technique of choice to analyse micro-residues remaining on prehistoric artefacts because of its very local (micron range) and non-destructive nature. It has been used successfully on lithics from different periods and locations [14, 23–26]. Other techniques such as Fourier Transform Infrared (FTIR) spectroscopy and Scanning Electron Microscopy coupled with Energy Dispersive X-rey Spectroscopy (SEM–EDS) have also been very useful to understand residues left on archaeological stone artefacts and replicates [27–31].

Here, we focus on seven stone artefacts from the older layers at Sibudu (from 71,000 to 77,000 years ago) using Raman spectroscopy and optical microscopy as non-destructive and non-invasive techniques to identify the residues on the stone surfaces. For comparison with these, we selected (from the same layers) sediments and ochre fragments showing traces of grinding. Their chemical signatures were compared with those of residues on the stone artefacts. Sediment samples were selected in order to investigate possible natural sources of residues on the artefacts. Worked ochre pieces were analysed with the same techniques in addition to FTIR to see whether traces from them could be detected on the grindstones.

Materials and methods

Samples

The specimens analysed here comprise seven stone artefacts from the Wadley excavations at Sibudu. Figure 1b shows the Sibudu stratigraphy including the layers from which the artefacts were found. A triangular fragment of grindstone and a flat pebble that was abraded on its circumference were excavated from layer Reddish-Grey Sand second scrape (RGS2) containing a Still Bay Industry (71,000 years ago). A polished stone is from Hearth 3 (H3) of layer Light Brownish-Grey (LBG, 72,500 years old). Four other artefacts come from the 77,000 year-old pre-Still Bay assemblage: first, a cortical flake found in the middle/base of Hearth 4 (H4), layer Brown Sand 7 (BS7), two grindstones from Brown Sand (BS) layer, and another grindstone from layer BS13.

Several ochre pieces were found in the same layers as the grindstones. Three ochre pieces found close to the artefacts, and showing use traces, were selected for the Raman analyses to compare their chemical signatures to the ones detected on the stone tools. Sb5186 was excavated near the triangular grindstone fragment and the pebble. Sb5167 is from layer RGS (brown 2) and Sb5383 was found near the cortical flake.

Sediment samples from RGS and RGS2 were previously analysed by Raman spectroscopy [14], and were not repeated here, but sediments, from various BS layers and LBG were analysed. The sediment samples from the squares B5c in the BS layer, C4a in BS13, C4b (H3) in LBG and B4a in BS where the other pre-Still Bay tools were found were unfortunately not available because they had been used for another analysis. Details of provenience for all the samples analysed are available in Table 1.

Methods

Optical microscopy and Raman micro-spectroscopy were successfully combined to identify residues on

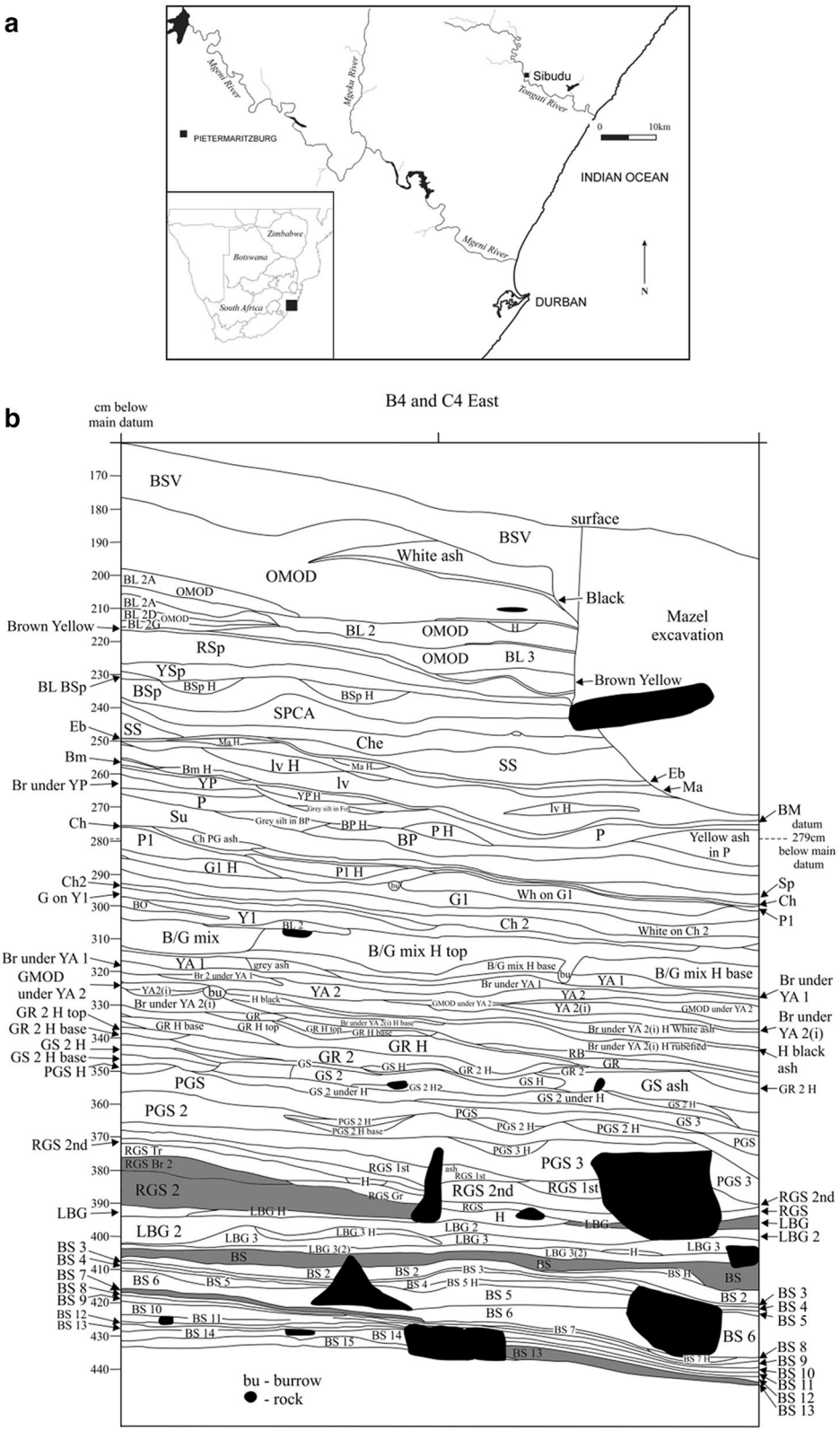

Fig. 1 **a** Sibudu locality and **b** Sibudu stratigraphy with the layers from which the tools come from highlighted in grey

Table 1 Contextual details of the samples

Sample name	Sample type	Lithic affiliation	Layer	Square
Pebble	Stone artefact	Still Bay	RGS2	C4d
Triangular grindstone	Stone artefact	Still Bay	RGS2	C4d
Sb5186	Ochre piece	Still Bay	RGS2	C4d
Sb5167	Ochre piece	Still Bay	RGS brown 2	B4a
Polished stone	Stone artefact	Pre-Still Bay	LBG (H3)	C4b
SbS-LBG-C4b	Sediment	Pre-Still Bay	LBG	C4b
SbS-LBG-C4a-H3(2)	Sediment	Pre-Still Bay	LBG (H3-2)	C4a
Grindstone	Stone artefact	Pre-Still Bay	BS	B4a
SbS-BS-H1-B4a	Sediment	Pre-Still Bay	BS (H1)	B4a
SbS-BS2-B4a	Sediment	Pre-Still Bay	BS2	B4a
Grindstone	Stone artefact	Pre-Still Bay	BS	B5c
Cortical flake	Stone artefact	Pre-Still Bay	BS7 (H4)	B4c
Sb5383	Ochre piece	Pre-Still Bay	BS7 (H4)	B4c
Sbs-BS7-B4c	Sediment	Pre-Still Bay	BS7	B4c
Broken slab-like grindstone	Stone artefact	Pre-Still Bay	BS13	C4a

BS brown sand, *H* hearth, *LBG* light brownish grey, *RGS* reddish grey sand

bifacial points [14] and on the younger Middle Stone Age grindstones mentioned earlier [23], and the method is repeated here. No preparation or cleaning of the artefacts was performed since it has been demonstrated that even rising with water removes some residue traces and can contaminate tools [28]. Throughout the study (including macro-photography and observations, microscopy and Raman measurements), the samples were at all times handled with powder-free latex gloves to avoid contamination from handling.

Optical microscopy

An Olympus BX63 upright microscope setup in reflective light mode with CellSens Dimension 1.12 software was used to observe and record images of the Still Bay and most of the pre-Still Bay artefacts (magnifications of 2× and 5×). Z-stacking was performed to combine all focal planes into a single focused image. Another Olympus instrument, a SZ61 Stereo Zoom Microscope with LED illumination stand and equipped with an Olympus DP12 microscope digital camera system, allowed photographing the cortical flake from the pre-Still Bay layer and the ochre piece Sb5383 (these were too large for the BX63 microscope's restricted space between the stage and the objectives).

Raman micro-spectroscopy

The molecular characterisation of the tools was performed using a LabRam HR800 spectrometer (Horiba–Jobin–Yvon) with an Olympus BX41 microscope attachment. The analyses were carried out with a 514.5 nm line of a Lexel argon ion laser focused through a 100× long working distance microscope objective (NA = 0.80); the power at the sample was kept under 0.2 mW to avoid any thermal photodecomposition [32]. For the sediment sample, it was possible to use a 100× objective (NA = 0.90) since the crushing of few milligrams of sample between two glass slides created a flat surface. A charged coupled detector cooled with liquid nitrogen collected the back-scattered Raman signal with a spectral resolution < 2 cm^{-1} between 80 and 1900 cm^{-1}. The integration times depended on the point of analysis and the level of fluorescence for obtaining a correct signal-to-noise ratio (ranging between 2 and 23 min). A total of 175 spectra was recorded for the study. After careful macroscopic and microscopic observations, areas on artefacts showing distinctive colours and textures were chosen and for each selected area, only one spectrum of each chemical compound was saved to avoid redundancy of results. Random areas on the tools were also analysed.

Infrared spectroscopy

FTIR spectroscopy measurements were performed on pieces Sb5167 and Sb5383 to demonstrate that they correspond to the ochre definition given previously. FTIR is, like Raman spectroscopy, a vibrational spectroscopy giving access to the molecular composition of the samples. Both techniques are complementary since some compounds can be Raman inactive, but detected with FTIR and vice versa. Micro-prelevements were performed on areas free of use traces and ground into a fine powder. The powder was then placed on the diamond crystal present on the Attenuated Total Reflectance (ATR) module of the Alpha (Bruker) portable spectrometer. The spectra

recorded are the result of 64 scans with a 4 cm^{-1} spectral resolution between 350 and 4000 cm^{-1}.

Results

Table 2 summarises the results of the Raman analyses performed on all the samples in addition to the attribution of the compounds detected on the samples and Table 3 the wavenumbers observed and their assignments.

Still Bay tools

Two tools are described here, a triangular fragment of grindstone and a flat pebble with an abraded circumference. Figure 2 presents the macro and micro-photographs of the grindstone fragment as well as the Raman spectra obtained on it. The grindstone exhibits multiple parallel striations on one side (see Fig. 2a upper) resulting from unidirectional rubbing against other material. The other side of the piece is irregular and rough (Fig. 2a lower) and was not ground. Multiple red, brown and dark/black stains are on both sides of the grindstone (Fig. 2b, c). These are haematite [33] (Fig. 2d spectrum A) often mixed with maghemite [23] (Fig. 2d spectrum B), which comprises two iron oxides with the same chemical formula, but different crystal structures: α-Fe_2O_3 (Rhombohedral lattice system) and γ-Fe_2O_3 (Spinel), respectively (see Table 3 for Raman band assignments). Most spectra show a mixture of the two compounds in different proportions (In total 14 spectra, one of pure haematite and six of pure maghemite). Sometimes additional bands were added to the mixture haematite/maghemite at around 663, 604, 578, 499 cm^{-1} (Fig. 2d spectrum D). These bands are characteristic of manganese oxides [34]. Numerous spectra of amorphous carbon [35] were recorded all over the grindstone, alone or in combination with quartz [36] (Fig. 2d spectrum C), haematite, maghemite and manganese oxide. Figure 2d spectrum E presents a spectrum of anatase [37] recorded on a white microscopic area located on a red stain; anatase was often recorded mixed with maghemite (see Fig. 2d spectrum B).

The macro and micro-photographs and the Raman spectra recorded on the pebble are shown in Fig. 3. One of the sides has a flake detached from it (Fig. 3a, right) and this could have resulted from tool use. Both sides of the pebble bear multiple residues, mainly beige ones, but also brown, red, black, white and grey. An example of a beige and brown micro-residue is visible on Fig. 3c. These residues are amorphous carbon (Fig. 3b spectrum A), haematite (Fig. 3b spectrum B) and anatase. The large black residue observable in Fig. 3d, produced spectra of amorphous carbon and maghemite (Fig. 3b spectrum E). The maghemite band intensity ratios are different from those recorded on the grindstone fragment maybe due to its low scattering properties and/or to its mixture with manganese oxides. Goethite (α-FeO(OH)) [33] (Fig. 3b spectrum F) was also identified on the pebble, near its edge. Only haematite and amorphous carbon were identified on the white residue (fluorescence prevented the recognition of other signals), and amorphous carbon combined with quartz (Fig. 3b spectrum D) in the dark grey areas. On black and reflective areas of the sample we obtained spectra of manganese oxides (Fig. 3b spectrum C) similar to those obtained on the grindstone fragment (at 663, 606, 572 and 495 cm^{-1}), but with a more intense signal and then showing additional bands at 393, 197 and 152 cm^{-1}.

During the Wadley excavations at Sibudu, 155 ochre pieces (of which 19 pieces show use traces) were recovered from the 71,000 year old layers. The piece named Sb5186 (Additional file 1: Figure S1) has rubbing use traces and was discovered near the two artefacts described here. It is a siltstone piece exhibiting medium hardness (between 3 and 4 on the Mohs scale), a silty/sandy grain size, and an orange (10R 5/8 on the Munsell colour chart) streak. The black/dark grey areas present on Sb5186 (Additional file 1: Figure S1a) were identified as manganese oxide with Raman spectroscopy (Additional file 1: Figure S1b spectrum A). The spectrum is however different from the ones recorded on the stone tools. By comparing the wavenumber attributions with other studies of iron oxides and oxyhydroxides, the vibrational bands observed can be attributed to a mixture of manganese and iron oxides and oxyhydroxides [38–40]. The analyses of Sb5186 also revealed the presence of amorphous carbon (Additional file 1: Figure S1b spectrum B) everywhere on the piece; goethite (Additional file 1: Figure S1b spectrum E) and haematite on the yellow, beige and red macro-areas, as well as anatase and quartz along with a haematite signal (Additional file 1: Figure S1b spectra D and C, respectively).

The Raman analyses of the sediments from the RGS2 layer at Sibudu revealed the presence of amorphous carbon, haematite, manganese oxide, anatase and calcite [14]. Calcite was not detected on the stone tools, but any of the other compounds could potentially have come from the sediments. Interestingly, goethite does not occur in the sediment, whereas it occurs on the ground pebble.

Goethite, anatase and manganese oxide were also identified in the utilised ochre sample, Sb5167 (Additional file 1: Figure S2). The piece, which has rubbed use wear traces, is soft (hardness lower than 2 on Mohs scale) snuffbox shale with a clayey grain size and a brownish-red streak (2.5YR 5/6 on the Munsell chart). The manganese oxide spectra recorded on Sb5167 have similar

Table 2 List of compounds detected on all the samples analysed with Raman micro-spectroscopy and their agent of accumulation

Age (year old)	Sample	Amorphous carbon	Quartz	Anatase	Haematite	Goethite	Maghemite	MnOx	Bone	Feldspar	Calcium carbonate
71,000	Pebble	x	x	x	x	x	x	x			
	Triangular grindstone	x	x	x	x		x	x			
	Sb5186	x	x	x	x	x		x			
	Sb5167	x		x		x					
72,500	Polished stone	x		x			x	x			
	SbS-LBG-C4b	x	x		x			x		x	
	SbS-LBG-C4a-H3(2)	x	x	x	x			x			
77,000	Grindstone BS B4a	x	x		x		x	x		x	
	SbS-BS-H1-B4a	x	x	x	x			x	x		x
	SbS-BS2-B4a	x	x	x	x			x			
	Grindstone BS B5c	x		x	x	x		x			
	Cortical flake	x			x	x		x			
	Sb5383	x			x			x			
	Sbs-BS7-B4c	x							x		
	Broken slab-like grindstone	x	x	x	x	x	x		x		
Compound origin on the stone tool		Sed/RC/UR/MA	Sed/RC/UR	Sed/RC/UR	Sed/RC/UR	UR	SM/UR	Sed/RC/UR/MA/SM	Sed	Sed/RC	Sed

MA micro-organism action, *MC* modern contamination, *RC* rock component, *Sed* sediments, *SM* secondary mineral, *UR* use residue

Table 3 Characteristic Raman features of the compounds detected on the samples

Name (chemical formula)	Band wavenumber (cm^{-1})	Figures	References
Anatase (TiO_2)	140–6, 399, 516, 636–41	2, 3, 4, 7, S1, S2, S3, S4, S5	[37]
Amorphous carbon (C)	1589–1616, 1357–79	2, 3, 4, 5, 6, 7, S1, S3, S4, S5, S6, S7	[35]
Bone hydroxyapatite (~$Ca_{10}(PO_4)_6(OH)_2$)	962	7, S5, S7	[25]
Calcium carbonate ($CaCO_3$)	1086	S5	[42]
Feldspar	107, 177, 265–8, 450–6, 475–8, 510–4, 650, 747–50, 812–3	5, S3	[41]
Goethite (α-FeO(OH))	93–5, 247–53, 299–309, 397–405, 480, 557–65, 649–61, 680–97	3, 6, 7, S1, S2, S4	[33]
Haematite (α-Fe_2O_3)	220–8, 243–7, 290–9, 403–14, 493–501, 604–17, 649–61, 1312–29	2, 3, 5, 6, 7, S1, S3, S4, S5, S6	[33]
Maghemite (γ-Fe_2O_3)	117, 197, 361, 497–501, 698–722, 1426	2, 3, 4, 5, 7	[23]
Manganese oxides	146–52, 195–208, 393–405, 495–505, 572–83, 600–15, 622–3, 658–70	2, 3, 5, 6, S2, S3, S4, S5, S6	[34]
	444, 501, 606, 654	4	
	203, 406, 501–7, 580–2, 643–9	4, S5	
	503, 561, 645	S3	
(Mixture manganese and iron oxides and oxyhydroxides)	142, 197, 290, 385, 427, 487–92, 534, 593, 649, 726, 1208	S1	
Quartz (SiO_2)	128–30, 206, 463–7	2, 3, 5, 7,	[36]

features (in term of band positions, intensity ratio and shape) to the ones recorded on the stone tools. The ATR-FTIR spectrum of Sb5167 (Additional file 1: Figure S2c) shows features of goethite and silicates which confirm that it is an ochre sample. Additional file 1: Table S1 summarises the assignments of the different ATR-FTIR bands.

Pre-Still Bay tools

A tool from Hearth 3 of layer LBG (72,500 years old) (Fig. 4) has one edge with striations (Fig. 4b) and many brown residues on its entire surface. Only amorphous carbon (Fig. 4d spectrum A), manganese oxides (Fig. 4d spectra B and C) and anatase (Fig. 4d spectrum D) were detected on this polished stone. This shows that haematite is not necessarily present on all tools even when haematite is present in the sediments surrounding them (Additional file 1: Figure S3). The spectrum presented in Fig. 4d spectrum C might contain attributes of maghemite (at 714 cm^{-1}).

The 77,000 year-old grindstone (from square B5c, layer BS) (Additional file 1: Figure S4) is an irregularly-shaped cobble with some polished surfaces. Over a large part of its surface there are stains in numerous shades of red, purple and dark grey. Many sediment particles remain on its surface comprising grey, brown and white deposits. Additional file 1: Figure S4c shows an enlargement of the features described. The compounds detected on the three artefacts previously described were also present on this grindstone except for maghemite and quartz. The manganese spectra were recorded on the darker areas of the specimen in association with amorphous carbon and anatase (Additional file 1: Figure S4b spectrum B). The vibrational bands are similar to those for manganese oxides detected on the other tools (Additional file 1: Figure S4b spectrum A). Haematite occurred on every area analysed on the tool. In some orange and red microscopic areas, spectra were recorded with mixtures of haematite and goethite, as well as amorphous carbon vibrations (Additional file 1: Figure S4b spectrum C). Only fluorescence signal could be retrieved on the white spots.

An artefact that appears to represent a broken, round, upper grindstone was found in layer BS (square B4a) and it is presented in Fig. 5 with the associated Raman spectra. The entire side of the grindstone fragment is polished (Fig. 5a left and c) and smeared with multiple red and black residues (Fig. 5a, b). The broken surface that was originally from inside the grindstone is rough and does not bear any use wear marks or residues, other than amorphous carbon and manganese oxide that were detected on both sides of the tool (Fig. 5d spectra A and E). The red residues present all over the polished surface are haematite (Fig. 5d spectrum B) sometimes mixed with maghemite (Fig. 5d spectrum F). One occurrence of haematite was also found on the broken surface near the edge of the tool, which may have continued to be used after it was broken. If so, ochre powder might have transferred from the active side to the inner edge while ochre processing was taking place. Quartz (Fig. 5d spectrum C) and feldspar [41] (Fig. 5d spectrum D) traces detected on

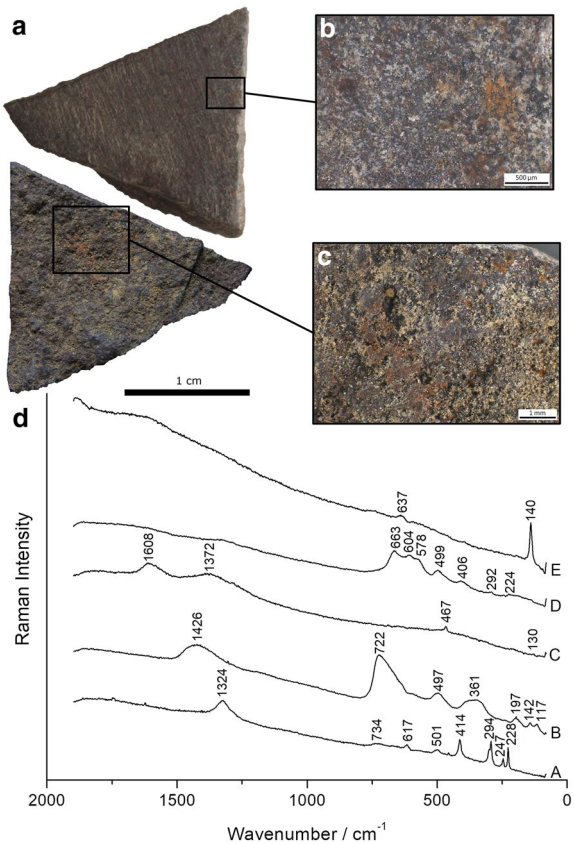

Fig. 2 **a** Photographs of both sides of the triangular grindstone fragment from layer RGS2 (square C4d); **b**, **c** high magnification images of residues exhibiting various red hues and **d** the characteristic Raman spectra obtained on the grindstone; (A) haematite, (B) maghemite and anatase (142 cm^{-1}), (C) amorphous carbon (1608 and 1372 cm^{-1}) and quartz (467 and 130 cm^{-1}), (D) manganese oxide and haematite (only the bands at 224, 292 and 406 cm^{-1} are observable) and (E) anatase

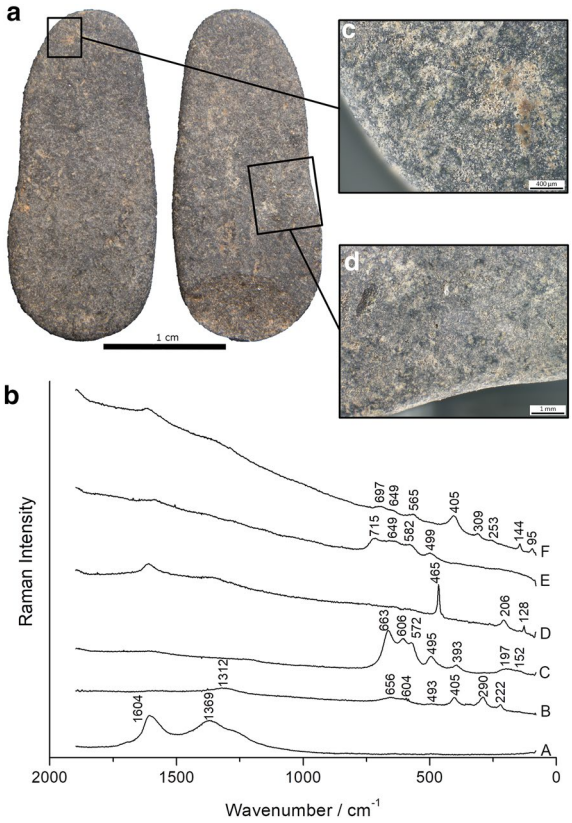

Fig. 3 **a** Photographs of both sides of the flat pebble from layer RGS2 (square C4d); **b** characteristic Raman spectra obtained on the pebble: (A) amorphous carbon, (B) haematite, (C) manganese oxide, (D) quartz, (E) maghemite mixed with manganese oxide and (F) goethite and anatase (144 cm^{-1}); **c** high magnification image of brown and beige residues and **d** high magnification image of beige, black and white residues

the broken face are attributed to the rock composition. Manganese oxide (Fig. 5d spectrum E) was detected on both surfaces with a chemical signature similar to the one recorded in the sediments (Additional file 1: Figure S5a spectrum D). Spectra presented in Additional file 1: Figure S5 belong to sediments recovered from close to where the artefact was excavated. Other than feldspar, which would have derived from the rock itself, all the compounds detected on the grindstone are also present in the sediments. Three additional compounds, not detected on the grindstone, were found in the sediments: anatase, phosphate [41] and calcium carbonate [42]. The absence of these three sediment components from the grindstone surface supports the conclusion that residues on the ground surface of the stone are most likely derived from ochre processing.

The large cortical flake from layer BS7 (77,000 years old) is not a grindstone. The dorsal side of the flake (see Fig. 6a top right) has two large impact scars perhaps resulting from percussion (the piece may be a broken hammerstone that was recycled), though they may be fire-popped scars because the piece was found in a hearth. The ventral side of this cortical flake has a large, thick, red residue (several centimetres wide and easily visible to the naked eye) pasted to it. Some black stains (a few millimetres in size) are scattered in and around the red residue (see Fig. 6a bottom left). Smaller red stains are spread around the large pasted residue (and on the sides of the flake) as well as some putative white fibres aligned parallel to each other (see Fig. 6c). Not surprisingly, the Raman analysis of the thick red residue identified amorphous carbon (Fig. 6b spectrum A) and haematite (Fig. 6b spectrum C). Orange areas visible microscopically on the red stain display goethite features (Fig. 6b spectrum D), and these are sometimes

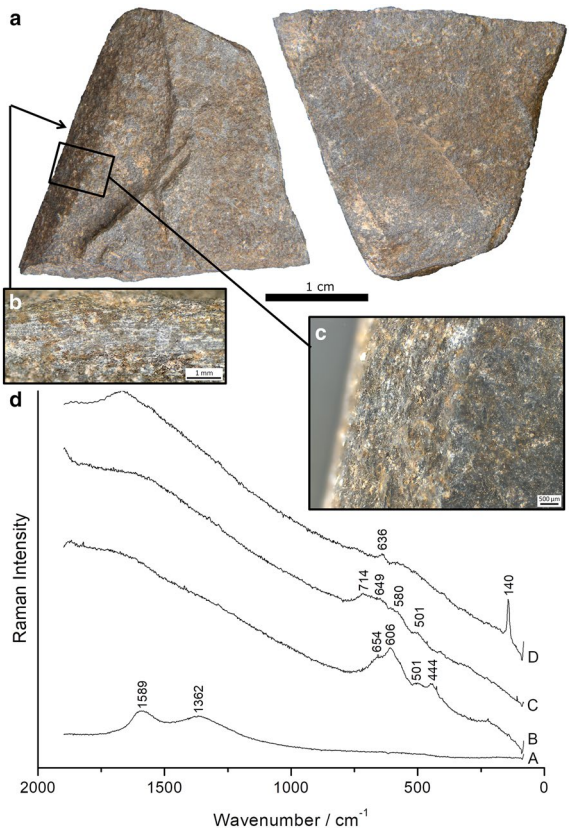

Fig. 4 **a** Photographs of the two faces of the polished stone excavated from Hearth 3 of layer LBG (square C4d); **b** micro-photograph showing striations on the polished edge; **c** examples of brown residues and **d** Raman spectra obtained on the grindstone: (A) amorphous carbon, (B) manganese oxide, (C) mixture of manganese oxide and maghemite and (D) anatase

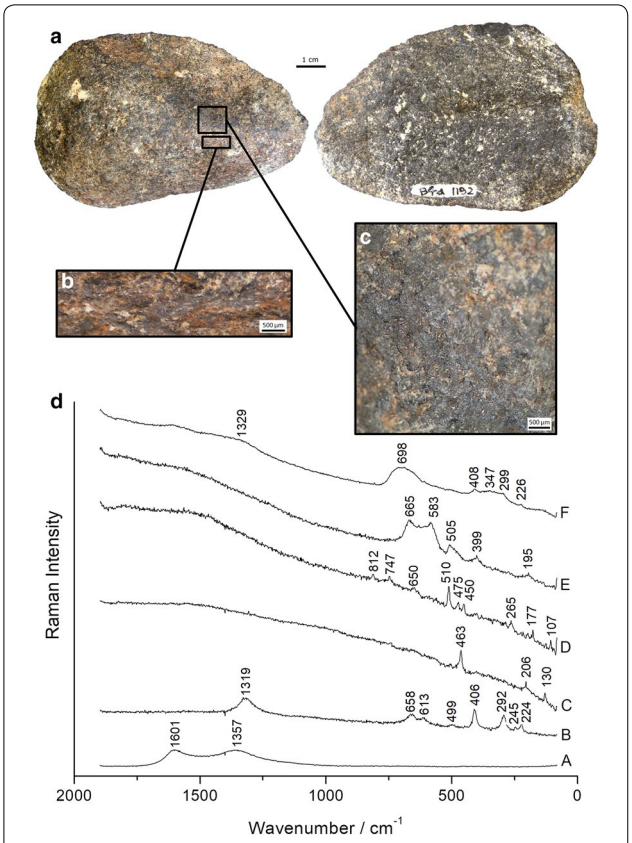

Fig. 5 **a** Both sides of the grindstone from layer BS square B4a; micro-photograph showing, **b** red residues and **c** smoothing features and **d** Raman spectra obtained on the grindstone: (A) amorphous carbon, (B) haematite, (C) quartz, (D) feldspar, (E) manganese oxide and (F) mixture of haematite and maghemite

mixed with haematite bands exhibiting various band intensity ratios. The white fibres discernible on the flake surface could not be identified by means of Raman spectroscopy either with 514 or 785 nm lines. They look like the silicified vegetal fibres formerly observed in silicified bedding construction also dated 77,000 years ago at Sibudu [43]. FT-IR spectroscopy may be able to characterise them, but this would necessitate their extraction from the flake, or the use of an instrument allowing reflectance micro-spectroscopy. Their identification would require the use of invasive and/or destructive techniques and we decided against these. Haematite was also recorded on this dorsal face and black stains are visible all over it. On both flake faces, the black stains are characterised by amorphous carbon and manganese oxide (Fig. 6b spectrum B). The manganese oxide spectra comprise bands around 146–8, 199, 397–9, 499–501, 580, 610–5, and 658–60 cm^{-1} and the stains are thus the same manganese species observed on the Still Bay tools.

The pre-Still Bay layers excavated during the Wadley campaign yielded 116 ochre pieces with 25 pieces exhibiting use wear traces. Sb5383, found near the cortical flake, is a 'snuff box' shale with medium hardness (Mohs 3 and 4), a clayey/silty grain size and a bright red (10R 3/6) streak (Additional file 1: Figure S6a). Ground striations are clearly seen on the edge of the piece (Additional file 1: Figure S6c). The Raman spectra recorded on the piece are haematite, amorphous carbon and manganese oxide, and the latter has a structure very close to the one present on the flake (Additional file 1: Figure S6b). ATR-FTIR spectroscopy recorded features of silicates, including quartz and kaolinite on the piece, validating it an ochre piece [44]. Chemical analysis using X-ray diffraction, portable X-ray fluorescence, SEM–EDS, FTIR and Raman spectroscopy performed on 26 ochre samples from the Sibudu collection showed a large variability in

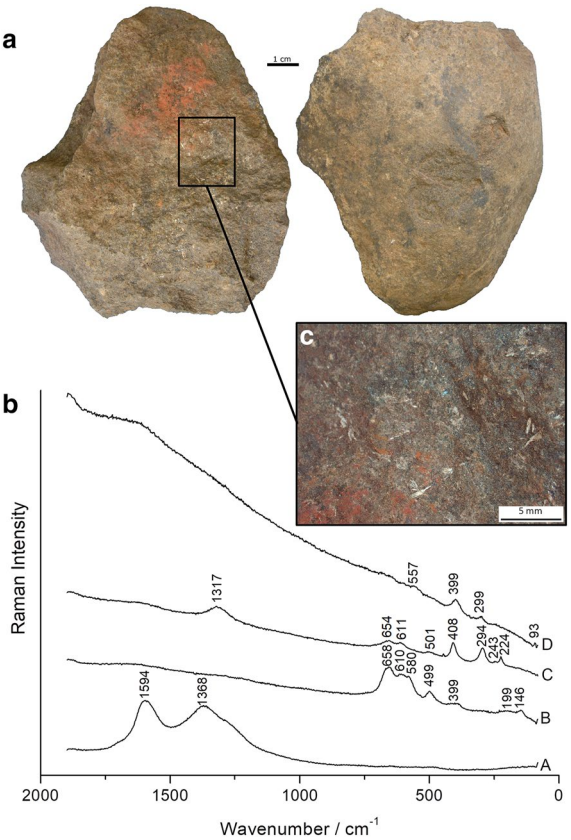

Fig. 6 **a** Photographs of the two faces of the cortical flake from layer BS7 (square B4c); **b** characteristic Raman spectra obtained on the flake: (A) amorphous carbon, (B) manganese oxide, (C) haematite, and (D) goethite and **c** high magnification image of red residues and white fibres

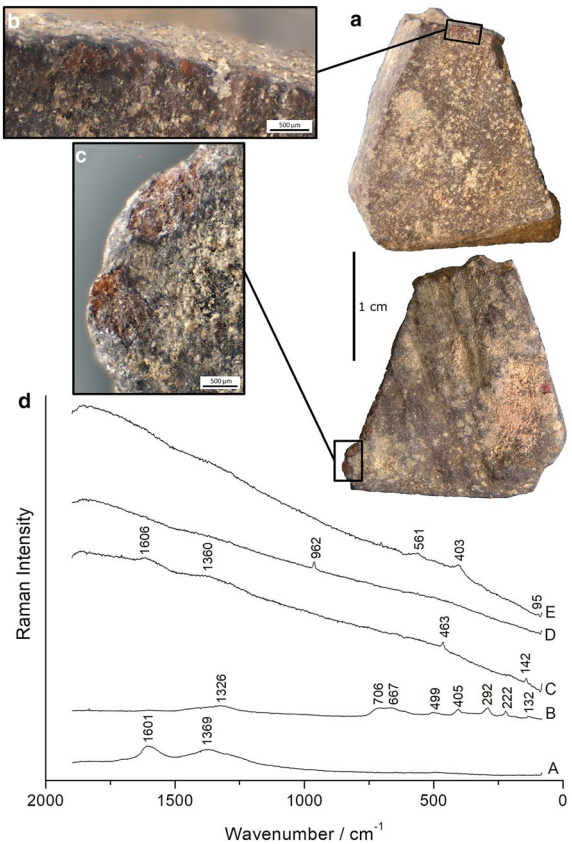

Fig. 7 **a** Photographs of the two sides of the flat grindstone recovered from layer BS13 (square C4a); **b**, **c** micro-photographs showing examples of red residues and **d** characteristic Raman spectra obtained on the grindstone: (A) amorphous carbon, (B) mixture of haematite and maghemite, (C) mixture of anatase, quartz and amorphous carbon, (D) phosphate and (E) goethite

term of mineralogical content [3, 22], explaining the differences observed on the other ochre pieces analysed.

The analysis of the sediments removed around the cortical flake showed the presence of amorphous carbon and the mineral part of bone with the PO_4 symmetric stretching vibration around 962 cm^{-1} (Additional file 1: Figure S7). A high fluorescence level prevented the detection of other compounds and this can be due to the presence of organic material such as humic acids [45].

The broken slab-like grindstone excavated from the layer BS13 is presented in Fig. 7. One thin edge (Fig. 7a top, top left of tool) has heavy striations suggesting that small precise grinding actions were carried out. The unused flat surface of one side of the grindstone (Fig. 7a top) has red residues on its edges (example Fig. 7b). The reverse side (Fig. 7a bottom) is curved and marked with deep grooves, and it also has red residues on its edges (Fig. 7c). Amorphous carbon was detected on both sides of the slab (Fig. 7d spectrum A). The red residues located on the edges comprise haematite, and in one instance haematite mixed with maghemite (Fig. 7d spectrum B). One spectrum of goethite (Fig. 6d spectrum E) and one spectrum of phosphate (Fig. 7d spectrum D) were recorded on random microscopic yellow and white spots, respectively. The goethite most probably comes from ochre processing and the phosphate from burnt bone fragments present in the sediments. Quartz and anatase (Fig. 7d spectrum C) were found on the unused side.

Discussion

The compounds detected on the Sibudu grindstones and other lithics by Raman spectroscopy may have originated from several sources, for example: (i) processing of materials in the past, (ii) rock composition, (iii) sediment adherence, (iv) contamination from handling by excavators and (v) the physical, chemical and biological changes which can occur from all these sources. The distinction between the different sources can sometimes be

ambiguous and several sources could be represented at the same time. Table 2 lists the occurrence of each compound. In the case of residues derived from deliberate processing, a combination of macro- and microscopic observations provides the most reliable interpretation, for example, use residues are most convincing when the matter is thickly spread or located in striations resulting from grinding activities.

Amorphous carbon was recorded on all the samples. It can be a component of ochre and then its presence on the sample can be due to use related activities. It is also a common compound found in rocks, representing vestiges of past bacterial activity, but it can also originate from carbon-rich fluid precipitation [46]. Amorphous carbon in the sediments can result from these processes in addition to organic matter degradation and to anthropogenic burning activity; certainly there is much evidence for fire use at Sibudu.

Anatase and quartz frequently merge with other compounds on Raman spectra acquired on rocks, as was also, for example, the case in the study of rock art from Patagonia [47] as well as for the previous studies of Sibudu tools [14, 23]. Anatase and quartz are also regularly found in sediments and they derive from rock decomposition [14, 23, 48–50]. Calcium carbonate and phosphate are common occurrences in hearths and probably result from the burning of vegetal matter and bone [51].

Only three samples didn't show traces of manganese oxides. Manganese oxides are present in the different types of sample (tools, ochre pieces and sediments) analysed and showed various Raman features mainly localised between 500 and 700 cm^{-1} characteristic of Mn–O and Mn–OH bending and stretching vibrations [52]. The wavenumber positions of the features recorded on the Still Bay pointed grindstone (Fig. 2d spectrum D) are similar to the ones obtained on metallic grey stains present on a grindstone dating 58,000 years ago at Sibudu made of manganese oxides [23]. The spectrum of these stains was attributed to a mixture of MnO_2 polymorphs and a hollandite-like structure ((Ba, K)(Mn, Ti, Fe)$_8O_{16}$) [34]. Even though manganese oxides have previously been recovered on Sibudu's stone tools [14, 23], they are unlikely to have been processed since no manganese oxide pieces were excavated at Sibudu and none has been found near the site. Ochre can contain manganese oxides [3] so ochre processing in addition to biotic and abiotic processes are potential sources of manganese oxide on the tools. Accidental accumulation is due to post-depositional diagenesis resulting from geochemical factors or micro-organism activity [53, 54]. Many factors influence the formation of manganese oxides such as the type of microorganism (heterotrophic, prosthecate or sheathed bacteria, fungi, algae also present in mixtures), the environmental conditions (pH, concentration, temperature) and the presence of other elements. Moreover, the large number of compounds that manganese can form in non-stoichiometric and disordered systems and the discrepancies in the Raman literature regarding their attribution make it difficult to interpret their formation processes on the samples. The large quantity of manganese oxide on the surface of the LBG stone tool might be an indicator of organic matter processing which promoted the development of micro-organism activity as was also hypothesised for a 58,000 year-old Sibudu grindstone, the surface of which was similarly covered by manganese oxides without any traces of haematite [23]. The presence of maghemite on the same specimen could have resulted from the heating of goethite present on it. Indeed it was recovered from a hearth and goethite transforms to maghemite when heated in the presence of organic matter, and this could have created the brown residues [55].

Differences can be noticed between the haematite spectra presented in Figs. 2, 3, 5 and 6 in term of band intensity ratio, band full width at half maximum, the extinction of the band at 247 cm^{-1}, and the appearance of a band at 656 cm^{-1}. They are attributed to differences in crystal stoichiometry and orientation. The band around 660 cm^{-1} is often attributed to magnetite (Fe_3O_4) in the literature [33, 55], or even to the presence of kaolinite [56], but it is clearly present on the xx polarisation configuration performed on a single haematite crystal at low laser power [57] and is then part of the haematite spectrum. This band is also considered dependent on the degree of crystallinity [47].

Ochre that varied by colour, shape and chemical composition was present throughout the Sibudu sequence and thousands of used and discarded pieces were excavated [22]. Ochre powder was produced with a variety of stone artefact types [58] and extensive patches of powder were recovered from some parts of the site [59]. Ochre was also found on some stone tools as a component of compound products like paint [15]. Here, multiple arguments favour the processing of ochre with the stone tools described. Replicated grinding shows that some ochre specimens have abrasive properties that cause grindstone wear [60, 61] and we hypothesise that the Still Bay triangular grindstone (RGS2-C4d—Fig. 2) may have been used this way. The detection, in the same layers, of identical compounds on both the ochre samples and the Still Bay stone artefacts is thus most likely due to the processing of ochre pieces. The 71,000 year old Still Bay assemblage has the highest percentage of yellow unutilised ochre (goethite) pieces in the whole Sibudu sequence [22]. In younger layers (dated ~ 58,000 years ago), powdered yellow and red ochre was found on cemented ash [59], and

red ochre was extensively ground with other materials on sandstone grindstones [23]. Goethite (with a yellow to brown streak) residues on the pebble described here (Fig. 3) most probably also came from ochre processing since goethite was not detected in the sediment samples, but instead occurs on the ochre specimens found in the same layer. The small size of the pebble and the presence of use wear and residues mainly on its thin edges imply that it was used for a fairly precise task, maybe for blending composites that included ochre. Pebbles bearing red and yellow ochre residues were also found in Middle Stone Age contexts at the Porc-Epic Cave in Ethiopia [4] and in early Middle Stone Age occupations in Sudan [62]. Rounded pebbles are generally considered to be upper grindstones [4] and the Sibudu Still bay pebble is likely to have been one. The triangular grindstone fragment (Fig. 2) exhibits numerous shades of red, brown and black all over its striations. These residues seem to be from grinding ochre, whereas the ochre residues on the other side of the specimen could have resulted from accidental transfer during the grinding process, for example by holding the piece with fingers stained by ochre powder.

Even though many sediment particles remain on the 77,000 year-old grindstone (B5c—layer BS) (Additional file 1: Figure S4), reddish residues of haematite sometimes mixed with goethite are also spread and smeared all over the stone suggesting a high probability that it was used in the *chaîne operatoire* of ochre processing. The large cortical flake (BS7 (H4) B4c) is hypothesised to have been used as a palette for the processing of an ochre-rich mixture that included plant material, but it is possible that the plant material is an incidental residue. The absence of bone signal on the cortical flake although bone is present in the surrounding sediment convinces us that the ochre paste on the flake did not originate from these sediments, but is likely to be a use-related residue.

Conclusions

The non-destructive methods used in this study reveal the presence of various compounds on seven lithic artefacts that were used in Sibudu between 77,000 and 71,000 years ago. Although haematite, goethite, maghemite, manganese oxides, amorphous carbon, quartz and anatase residues can originate within the rock from which the artefact is made, or within site sediment as a result of rock decomposition, they can also be a by-product of ochre processing which was undoubtedly carried out at the site. The prominent presence of thick ochre (haematite and goethite) residues pasted on artefacts, as is the case with the 77,000 year-old cortical flake and the large smoothed grindstone, seems to demonstrate ochre processing by people, particularly since bone residues that are components of the sediment are absent from the ochre paste. We are confident that the large red stain on the ventral surface of the cortical flake results from crushing and/or grinding of ochre on its surface. Thinner ochre residues spread on four of the other lithics may also be the result of ochre powder processing, but the level of certainty is not as high. The manganese oxide stains that we observed may sometimes be due to natural biotic or abiotic processes, and this seems particularly likely when they occur in heavy concentrations all over a tool. Manganese oxide can, however, be a natural ochre inclusion, so the compound can occasionally come from ochre processing. Goethite and maghemite might, like haematite residues, sometimes come from the degradation of rocks, so we are cautious with our interpretations of ochre processing from these two products. We are also aware that sediments may accidentally coat stone tools in a site, so we characterised the sediments from each layer where tools were found. While many of the compounds we find on the stone tools also occur in the sediments, we are encouraged to interpret an ochre residue as use-related when it lacks some of the compounds or products like crushed bone that are common in sediment.

Where we can demonstrate use on the artefacts described here, the tools appear to have been used for mixing ochre-rich products, or for the crushing, pounding and/or grinding of ochre pieces most probably in order to create powder. During the 77,000 to 71,000 year old pre-Still Bay and Still Bay occupations at Sibudu we did not find other materials processed with these old grindstones. This is a different situation from that at 58,000 years ago where grindstones were used for processing a range of products, including bone [23]. The composition of the ochre found on the 77,000 to 71,000 year old stone tools includes a range of iron oxide and oxyhydroxides (haematite, maghemite and goethite). The processing of goethite seems to have ceased by 58,000 years ago because it was not found on the younger grindstones notwithstanding that these yielded residues from a range of materials [23]. Thus our grindstone study not only describes processing of ochre at Sibudu, and change in the types of ochre favoured through time, but it has demonstrated changing patterns in the use of grindstones and increasing diversity of materials processed with them in more recent occupations.

Additional file

Additional file 1. Additional figures and table.

Abbreviations

RGS2: reddish-grey sand second scrape; H: hearth; BS: brown sand; LBG: light brownish grey; LED: light-emitting diode; NA: numerical aperture; MA:

micro-organism action; MC: modern contamination; RC: rock component; Sed: sediments; SM: secondary mineral; UR: use residue.

Authors' contributions
LW excavated and selected the stone tools, ochre and sediment samples, performed the preliminary macro- and microscopic examinations of the samples, and reviewed and edited the manuscript. MW selected the ochre and sediment samples, took the macro- and micro-pictures, carried out the Raman and FTIR analysis, treated the data and drafted the manuscript. Both authors read and approved the final manuscript.

Acknowledgements
The authors acknowledge the Microscopy and Microanalysis Unit (University of the Witwatersrand) for the use of the optical microscope and the Raman spectrometer. Tammy Hodgskiss is thanked for sharing her detailed database of the Sibudu ochre collection from the Wadley excavations.

Competing interests
The authors declare that they have no competing interests.

Availability of data and materials
The datasets used and/or analysed during the current study are available from the corresponding author on reasonable request. All the materials analysed for the study are being curated at the Evolutionary Studies Institute, University of the Witwatersrand, Johannesburg.

Funding
MW's post-doctoral fellowship and research is funded by the Research Office of the University of the Witwatersrand. Research funding was provided to LW by the National Research Foundation (NRF) of South Africa. The NRF is not responsible for and does not necessarily support the interpretations reached by the authors.

Permission to excavate
The excavations at Sibudu were undertaken with heritage permit (Number 007/09) issued by the South African heritage agency responsible for KwaZulu-Natal, Amafa KwaZulu-Natali.

Publisher's Note

Received: 21 January 2019 Accepted: 17 April 2019
Published online: 24 May 2019

References

1. Watts I. Ochre in the Middle Stone Age of southern Africa: ritualised display or hide preservative? S Afr Archaeol Bull. 2002;57:1–14.
2. Wadley L. Ochre crayons or waste products? Replications compared with MSA 'crayons' from Sibudu Cave, South Africa. Before Farm. 2005;2005:1–12.
3. Wojcieszak M, Hodgskiss T, Colomban P, Wadley L. Chapter 41: Finding Chemical and physical evidence of heat treatment of ochre by using non-destructive methods: a preliminary study. In: Pereira T, Terradas X, Bicho N, editors. The raw materials exploitation in prehistory: sourcing, processing and distribution. Newcastle: Cambridge Scholars Publishing; 2017. p. 587–600.
4. Rosso DE, Pitarch Martí A, d'Errico F. Middle Stone Age ochre processing and behavioural complexity in the horn of Africa: evidence from porcepic Cave, Dire Dawa, Ethiopia. PLoS ONE. 2016;11:e0164793.
5. Dayet L, Texier PJ, Daniel F, Porraz G. Ochre resources from the Middle Stone Age sequence of Diepkloof Rock Shelter, Western Cape, South Africa. J Archaeol Sci. 2013;40:3492–505.
6. Henshilwood CS, d'Errico F, Watts I. Engraved ochres from the Middle Stone Age levels at Blombos Cave, South Africa. J Hum Evol. 2009;57:27–47.
7. Hodgskiss T. Ochre use in the Middle Stone Age at Sibudu, South Africa: grinding, rubbing, scoring and engraving. J Afr Archaeol. 2013;11:75–95.
8. Couraud C. Les pigments des grottes d'Arcy-sur-Cure (Yonne). Gallia Préhistoire. 1991;33:17–52.
9. Rifkin RF. Assessing the efficacy of red ochre as a prehistoric hide tanning ingredient. J Afr Archaeol. 2011;9:131–58.
10. Mahaney WC, Hancock RGV, Inoue M. Geochemistry and clay mineralogy of soils eaten by Japanese macaques. Primates. 1993;34:85–91.
11. Ellis LWS, Caran C, Glascock MD, Tweedy SW, Neff H. Appendix H: Geochemical and mineralogical characterization of ocher from an archaeological context. Hot rock cooking on the greater edwards plateau four burned rock midden sites in West Central Texas. Austin Texas: Texas Archaeological Research Laboratory, University of Texas - Studies in Archaeology; 1997.
12. Velo J. Ochre as medicine: a suggestion for the interpretation of the archaeological record. Curr Anthropol. 1984;25:674.
13. Lombard M. Direct evidence for the use of ochre in the hafting technology of Middle Stone Age tools from Sibudu Cave. S Afr Humanit. 2006;18:57–67.
14. Wojcieszak M, Wadley L. Raman spectroscopy and scanning electronic microscopy confirm ochre residues on 71,000 year old bifacial tools from Sibudu, South Africa. Archaeometry. 2018;60:1062–76.
15. Villa P, Pollarolo L, Degano I, Birolo L, Pasero M, Biagioni C, et al. A milk and ochre paint mixture used 49,000 years ago at Sibudu, South Africa. PLoS ONE. 2015;10:e0131273.
16. Henshilwood CS, d'Errico F, van Niekerk KL, Coquinot Y, Jacobs Z, Lauritzen S-E, et al. A 100,000-year-old ochre-processing workshop at Blombos Cave, South Africa. Science. 2011;334:219–22.
17. Rifkin RF, Dayet L, Queffelec A, Summers B, Lategan M, d'Errico F. Evaluating the photoprotective effects of ochre on human skin by *In Vivo* SPF assessment: implications for human evolution, adaptation and dispersal. PLoS ONE. 2015;10:e0136090.
18. Henshilwood CS, d'Errico F, van Niekerk KL, Dayet L, Queffelec A, Pollarolo L. An abstract drawing from the 73,000-year-old levels at Blombos Cave, South Africa. Nature. 2018;562:115–8.
19. Bonneau A, Pearce D, Mitchell P, Staff R, Arthur C, Mallen L, et al. The earliest directly dated rock paintings from southern Africa: new AMS radiocarbon dates. Antiquity. 2017;91:322–33.
20. Wadley L, Jacobs Z. Sibudu Cave: background to the excavations, stratigraphy and dating. S Afr Humanit. 2006;18:1–26.
21. Jacobs Z, Wintle AG, Duller GAT, Roberts RG, Wadley L. New ages for the post-Howiesons Poort, late and final Middle Stone Age at Sibudu, South Africa. J Archaeol Sci. 2008;35:1790–807.
22. Hodgskiss T. An investigation into the properties of the ochre from Sibudu, KwaZulu-Natal, South Africa. S Afr Humanit. 2012;24:99–120.
23. Wojcieszak M. Material processed with 58,000-year-old grindstones from Sibudu (KwaZulu-Natal, South Africa) identified by means of Raman microspectroscopy. J Raman Spectrosc. 2018;49:830–41.
24. Bordes L, Fullagar R, Prinsloo L, Hayes E, Kozlikin M, Shunkov M, et al. Raman spectroscopy of lipid micro-residues on Middle Palaeolithic stone tools from Denisova Cave, Siberia. J Archaeol Sci. 2018. https://doi.org/10.1016/j.jas.2018.05.00.
25. Bordes L, Prinsloo LC, Fullagar R, Sutikna T, Hayes E, Jatmiko, et al. Viability of Raman microscopy to identify micro-residues related to tool-use and modern contaminants on prehistoric stone artefacts. J Raman Spectrosc. 2017;48:1212–21.
26. Croft S, Chatzipanagis K, Kröger R, Milner N. Misleading residues on lithics from Star Carr: identification with Raman microspectroscopy. J Archaeol Sci Rep. 2018;19:430–8.
27. Hayes E, Cnuts D, Rots V. Integrating SEM-EDS in a sequential residue analysis protocol: benefits and challenges. J Archaeol Sci Rep. 2019;23:116–26.
28. Hayes E, Rots V. Documenting scarce and fragmented residues on stone tools: an experimental approach using optical microscopy and SEM-EDS. Archaeol Anthropol Sci. 2018. https://doi.org/10.1007/s12520-018-0736-1.
29. Monnier G, Frahm E, Luo B, Missal K. Developing FTIR microspectroscopy for the analysis of animal-tissue residues on stone tools. J Archaeol Method Theory. 2018;25:1–44.

30. Prinsloo LC, Wadley L, Lombard M. Infrared reflectance spectroscopy as an analytical technique for the study of residues on stone tools: potential and challenges. J Archaeol Sci. 2014;41:732–9.
31. Rots V, Hayes E, Cnuts D, Lepers C, Fullagar R. Making sense of residues on flaked stone artefacts: learning from blind tests. PLoS ONE. 2016;11:e0150437.
32. Cvejic Z, Rakic S, Kremenovic A, Antic B, Jovalekic C, Colomban P. Nanosize ferrites obtained by ball milling: crystal structure, cation distribution, size-strain analysis and Raman investigations. Solid State Sci. 2006;8:908–15.
33. de Faria DLA, Venâncio Silva S, de Oliveira MT. Raman microspectroscopy of some iron oxides and oxyhydroxides. J Raman Spectrosc. 1997;28:873–8.
34. Julien CM, Massot M, Poinsignon C. Lattice vibrations of manganese oxides: part I. Periodic structures. Spectrochim Acta Mol Biomol Spectrosc. 2004;60:689–700.
35. Prinsloo LC, Tournié A, Colomban P, Paris C, Bassett ST. In search of the optimum Raman/IR signatures of potential ingredients used in San/Bushman rock art paint. J Archaeol Sci. 2013;40:2981–90.
36. Sato RK, McMillan PF. An infrared and Raman study of the isotopic species of alpha-quartz. J Phys Chem. 1987;91:3494–8.
37. Ohsaka T, Izumi F, Fujiki Y. Raman spectrum of anatase, TiO_2. J Raman Spectrosc. 1978;7:321–4.
38. Barbosa AL, Jimenez C, Mosquera JA. Detection of iron phases presents in archaeological artifacts by Raman spectroscopy. Corros Sci Technol. 2018;17:60–7.
39. Kuebler KE. A comparison of the iddingsite alteration products in two terrestrial basalts and the Allan Hills 77005 martian meteorite using Raman spectroscopy and electron microprobe analyses. J Geophys Res Planets. 2013;118:803–30.
40. Neff D, Bellot-Gurlet L, Dillmann P, Reguer S, Legrand L. Raman imaging of ancient rust scales on archaeological iron artefacts for long-term atmospheric corrosion mechanisms study. J Raman Spectrosc. 2006;37:1228–37.
41. Freeman JJ, Wang A, Kuebler KE, Jolliff BL, Haskin LA. Characterization of natural feldspars by Raman spectroscopy for future planetary exploration. Can Mineral. 2008;46:1477–500.
42. Tomić Z, Makreski P, Gajić B. Identification and spectra-structure determination of soil minerals: raman study supported by IR spectroscopy and X-ray powder diffraction. J Raman Spectrosc. 2010;41:582–6.
43. Wadley L, Sievers C, Bamford M, Goldberg P, Berna F, Miller C. Middle Stone Age bedding construction and settlement patterns at Sibudu, South Africa. Science. 2011;334:1388–91.
44. Moyo S, Mphuthi D, Cukrowska E, Henshilwood CS, van Niekerk K, Chimuka L. Blombos Cave: Middle Stone Age ochre differentiation through FTIR, ICP OES, ED XRF and XRD. Quat Int. 2015. https://doi.org/10.1016/j.quaint.2015.09.041.
45. Edwards H, Munshi T, Scowen I, Surtees A, Swindles GT. Development of oxidative sample preparation for the analysis of forensic soil samples with near-IR Raman spectroscopy. J Raman Spectrosc. 2012;43:323–5.
46. Bower DM. Micro-Raman spectroscopic investigations of mineral assemblages in parallel to bedding laminae in 2.9 Ga sandstones of the Pongola Supergroup, South Africa. J Raman Spectrosc. 2010;42:1626–33.
47. Rousaki A, Vargas E, Vázquez C, Aldazábal V, Bellelli C, Carballido Calatayud M, et al. On-field Raman spectroscopy of Patagonian prehistoric rock art: pigments, alteration products and substrata. Trends Analyt Chem. 2018;105:338–51.
48. Anthony JW, Bideaux RA, Bladh KW, Nichols MC. Handbook of mineralogy. Tucson Arizona: Mineral Data Publishing; 1990.
49. Bonneau A, Pearce DG, Pollard AMA. A multi-technique characterization and provenance study of the pigments used in San rock art, South Africa. J Archaeol Sci. 2012;39:287–94.
50. Wadley L. Putting ochre to the test: replication studies of adhesives that may have been used for hafting tools in the Middle Stone Age. J Hum Evol. 2005;49:587–601.
51. Schiegl S, Stockhammer P, Scott C, Wadley L. A mineralogical and phytolith study of the Middle Stone Age hearths in Sibudu Cave, KwaZulu-Natal, South Africa: Sibudu Cave. S Afr J Sci. 2004;100:185–94.
52. Ospitali F, Smith DC, Lorblanchet M. Preliminary investigations by Raman microscopy of prehistoric pigments in the wall-painted cave at Roucadour, Quercy, France. J Raman Spectrosc. 2006;37:1063–71.
53. Greene AC, Madgwick JC. Microbial formation of manganese oxides. Appl Environ Microbiol. 1991;57:1114–20.
54. Vodyanitskii YN, Vasilev AA, Lesovaya SN, Sataev EF, Sivtsov AV. Formation of manganese oxides in soils. Eur Soil Sci Pochvovedenie. 2004;37:572–84.
55. Maguregui M, Castro K, Morillas H, Trebolazabala J, Knuutinen U, Wiesinger R, et al. Multianalytical approach to explain the darkening process of hematite pigment in paintings from ancient Pompeii after accelerated weathering experiments. Anal Methods. 2014;6:372–8.
56. Bikiaris D, Daniilia S, Sotiropoulou S, Katsimbiri O, Pavlidou E, Moutsatsou AP, et al. Ochre-differentiation through micro-Raman and micro-FTIR spectroscopies: application on wall paintings at Meteora and Mount Athos, Greece. Spectrochim Acta Mol Biomol Spectrosc. 2000;56:3–18.
57. Bersani D, Lottici PP, Montenero A. Micro-Raman investigation of iron oxide films and powders produced by sol–gel syntheses. J Raman Spectrosc. 1999;30:355–60.
58. Williamson BS. Middle Stone Age tool function from residue analysis at Sibudu Cave: Sibudu Cave. S Afr J Sci. 2004;100:174–8.
59. Wadley L. Cemented ash as a receptacle or work surface for ochre powder production at Sibudu, South Africa, 58,000 years ago. J Archaeol Sci. 2010;37:2397–406.
60. Dubreuil L. Functional studies of prehistoric grindingstones. Bull Centre Recherche Français Jérusalem. 2001;9:73–87.
61. Hodgskiss T. Identifying grinding, scoring and rubbing use-wear on experimental ochre pieces. J Archaeol Sci. 2010;37:3344–58.
62. Van Peer P, Rots V, Vroomans J-M. A story of colourful diggers and grinders: the Sangoan and Lupemban at site 8-B-11, Sai Island, Northern Sudan. Before Farm. 2004;2004:1–28.